JOURNAL OF CELLULAR PHYSIOLOGY 184:263–274 (2000)

Lysosomal Accumulation of Drugs in Drug-Sensitive MES-SA but Not Multidrug-Resistant MES-SA/Dx5 Uterine Sarcoma Cells

EXING WANG, MICHELE D. LEE, AND KENNETH W. DUNN*

Department of Medicine, Indiana University School of Medicine, Indianapolis, Indiana

Sequestration of drugs in intracellular vesicles has been associated with multidrug-resistance (MDR), but it is not clear why vesicular drug accumulation, which depends upon intracellular pH gradients, should be associated with MDR. Using a human uterine sarcoma cell line (MES-SA) and a doxorubicin (DOX)-resistant variant cell line (Dx-5), which expresses p-glycoprotein (PGP), we have addressed the relationship between multidrug resistance, vesicular acidification, and vesicular drug accumulation. Consistent with a pH-dependent mechanism of vesicular drug accumulation, studies of living cells vitally labeled with multiple probes indicate that DOX and daunorubicin (DNR) predominately accumulate in lysosomes, whose lumenal pH was measured at < 4.5, but are not detected in endosomes, whose pH was measured at 5.9. However, vesicular DOX accumulation is more pronounced in the drug-sensitive MES-SA cells and minimal in Dx5 cells even when cellular levels of DOX are increased by verapamil treatment. While lysosomal accumulation of DOX correlated well with pharmacologically induced differences in lysosome pH in MES-SA cells, lysosomal accumulation was minimal in Dx5 cells regardless of lysosomal pH. We found no differences in the pH of either endosomes or lysosomes between MES-SA and Dx5 cells, suggesting that, in contrast to other MDR cell systems, the drug-resistant Dx5 cells are refractory to pH-dependent vesicular drug accumulation. These studies demonstrate that altered endomembrane pH regulation is not a necessary consequence of cell transformation, and that vesicular sequestration of drugs is not a necessary characteristic of MDR. J. Cell. Physiol. 184:263–274, 2000.

One of the primary obstacles in cancer chemotherapy is the development of multi-drug resistance (MDR) by tumor cells. Cells that acquire MDR are characterized by decreased accumulation of a variety of drugs. MDR is a generic property in that different MDR cell lines show different morphological, physiological, and biochemical modifications. As such, it is probably accomplished by a variety of different mechanisms in different MDR cells. Initially associated with expression of PGP (Endicott and Ling, 1989; Gottesman and Pastan, 1993), MDR has now been associated with at least two other related proteins, MDR-related protein (MRP, [Cole et al., 1992] and a 110 kD lysosomal protein [Scheper et al., 1993]). All of these proteins are members of the ATP-Binding Cassette (ABC) family of proteins, which are frequently ATP-driven membrane transporters. This homology with ABC transporters suggests a model of MDR in which PGP utilizes energy from ATP to pump drugs out of the cytosol or out of the plasma membrane bilayer against a concentration gradient. However, it has also been suggested that reduced intracellular drug accumulation might result from biophysical changes that accompany MDR, specifically decreased transmembrane pH gradients or electrical potentials (reviewed by Simon and Schindler [1994]; Wadkins and Roepe [1997]).

An alternative model involves the role of endomembrane compartments in MDR (reviewed by Simon and Schindler [1994]). Fluorescent drugs that are found in the nucleus and diffusely labeling the cytoplasm of sensitive cells are frequently found in peri-nuclear punctate vesicles in resistant cells (Beck, 1987; Klohs and Steinkampf, 1988; Gervasoni et al., 1991; de Lange et al., 1992; Rutherford and Willingham, 1993; Altan et al., 1998; Shapiro et al., 1998). Many studies have demonstrated an association between vesicular drug distributions and the expression of PGP (Gervasoni et al., 1991; Sognier et al., 1992; Sognier et al., 1994; Seidel et al., 1995; Cleary et al., 1997; Altan et al., 1998; Shapiro et al., 1998), or MRP (Breuninger et al.,

Contract grant sponsor: American Cancer Society; Contract grant number: IRG-161-K; Contract grant sponsor: NIH; Contract grant number: R29DK51098.

*Correspondence to: Kenneth W. Dunn, Department of Medicine, Indiana University School of Medicine, 1120 South Drive FH115, Indianapolis, IN 46202-5116. E-mail: kwdunn@iupui.edu

Received 4 November 1999; Accepted 13 March 2000

1995) although drugs have also been observed in vesicles of sensitive cells (Willingham et al., 1986; Lelong et al., 1991; Lautier et al., 1997). Sequestration of drugs in endomembrane compartments may confer some degree of protection on cells from the effects of drugs whose cytotoxic targets are cytoplasmic or nuclear (Sognier et al., 1994; Breuninger et al., 1995). Drugs may also be effluxed via exocytosis (Klohs and Steinkampf, 1988; Warren et al., 1991; Seidel et al., 1995), providing another mechanism of protection.

The presence of PGP and its 110 kD homologue on intracellular vesicles (Scheper et al., 1993; Simon and Schindler, 1994; Kim et al., 1997) suggests that drugs may be actively transported into endomembrane compartments in MDR cells, and there is some evidence that supports a model of active pumping of drugs by PGP in endomembranes (Shapiro et al., 1998). However, significant evidence indicates that vesicular accumulation depends upon the transmembrane pH gradient of intracellular organelles. Many cytotoxic drugs are basic, and in their uncharged, hydrophobic form diffuse across lipid bilayers relatively freely. Upon becoming protonated in acidic compartments, however, these drugs would be rendered hydrophilic and become trapped. This phenomenon provides the basis for a model of drug resistance in MDR cells, called the PSS model (Schindler et al., 1996; Altan et al., 1998), in which weakly basic drugs become *P*rotonated in acidic organelles, in which they are *S*equestered and ultimately *S*ecreted from the cell.

Consistent with this mechanism, the vesicles in which drugs accumulate have been identified as lysosomes (Warren et al., 1991; Hurwitz et al., 1997; Altan et al., 1998), endosomes (Altan et al., 1998), and vesicles of the Golgi compartment (Klohs and Steinkampf, 1988; Lautier et al., 1997; Altan et al., 1998), all of which are acidic organelles. Furthermore, treatments known to increase the pH of endomembrane compartments block vesicular accumulation of drugs (Willingham et al., 1986; Beck, 1987; Klohs and Steinkampf, 1988; Moriyama et al., 1994; Cleary et al., 1997; Hurwitz et al., 1997; Altan et al., 1998) and block cellular drug efflux (Marquardt and Center, 1991).

The pH-dependent accumulation of drugs in vesicles has been correlated with expression of PGP (Cleary et al., 1997; Altan et al., 1998), but the precise role of PGP in this accumulation is unclear. Although it has been demonstrated that PGP activity is independent of transmembrane pH gradients (Ruetz and Gros, 1994), there are several ways in which MDR cells might specifically exploit acidification-dependent vesicular accumulation of drugs to enhance drug resistance. First, sequestration of drugs may be increased by the increased volume of the elaborated endosome/lysosome system frequently observed in MDR cells (Zamora and Beck, 1986; Sognier et al., 1994; Hurwitz et al., 1997). Second, drug efflux might be enhanced by the increased rates of exocytosis that have been reported in several MDR cell lines (Sehested et al., 1987a; Sehested et al., 1987b; Warren et al., 1991). Finally, there is increasing evidence that both sequestration and efflux may be enhanced in MDR cells by increasing the efficiency of drug transport into vesicular compartments by increasing their transmembrane pH gradients.

But rather than increasing pH gradients beyond those found in normal cells, it appears that expression of PGP rescues a lesion found in transformed cells. Several studies indicate that transformed cells manifest decreases in cytosolic pH (Keizer and Joenje, 1989; Boscoboinik et al., 1990; Thiebaut et al., 1990; Roepe, 1992; Luz et al., 1994; Hoffman et al., 1996; Schindler et al., 1996; Altan et al., 1998) and increases in vesicular pH (Schindler et al., 1996; Millot et al., 1997; Altan et al., 1998), changes that would reduce the transmembrane pH gradient of intracellular organelles, and thus block vesicular accumulation. Corresponding drug-resistant clones derived from these cells display normal cytosolic and vesicular pH regulation. Although this acidification-dependent model of PGP action provides a satisfying explanation for the otherwise puzzling diversity of PGP "substrates", it is not clear why pH regulation is altered in tumor cells, nor why pH regulation is rescued in MDR cells. Increased vesicular acidification in MDR cells may derive from overexpression of endosome/lysosome proton pumps (Ma and Center, 1992), or from the Cl^- channel activity of PGP (Valverde et al., 1992) in vesicle membranes, which could enhance vesicular acidification by providing a counterion current, as is required for endosome acidification (Van Dyke, 1986; Barasch et al., 1988; Fuchs et al., 1989; Bae and Verkman, 1990; Zen et al., 1992).

Using a human uterine sarcoma cell line (MES-SA) (Harker et al., 1983) and a doxorubicin-selected derivative cell line (Dx5) (Harker and Sikic, 1985), we have addressed the relationship between multidrug resistance, vesicular acidification, and vesicular drug accumulation. The Dx5 cells are cross-resistant to a variety of drugs (Harker et al., 1986; Gosland et al., 1993; Lau et al., 1994; Gosland et al., 1996; Chen et al., 1997; Dumontet et al., 1998), and this cross-resistance is correlated with the expression of PGP (Gosland et al., 1989; Luckie et al., 1996; Chen et al., 1997), but not MRP (Chen et al., 1997). The increased resistance of the Dx5 cells has been correlated with a reduced cellular accumulation of drugs (Lau et al., 1994; Dumontet et al., 1998). Our studies demonstrate that vesicular accumulation of DOX or daunorubicin is predominately restricted to lysosomes in both cell lines. However, to our surprise we found that vesicular drug accumulation is much more pronounced in the parental tumor cell line and minimal in the MDR variant cells even when cellular levels of DOX are increased by verapamil treatment. While lysosomal accumulation of DOX correlated well with pharmacologically induced differences in lysosome pH in MES-SA cells, lysosomal accumulation was minimal regardless of lysosomal pH in Dx5 cells. Significantly, the pH of both endosomes and lysosomes are similar in Dx5 and MES-SA cells for all experimental conditions, suggesting that, in contrast to other MDR cell systems, drug-resistant Dx5 cells are refractory to pH-dependent vesicular drug accumulation. These studies indicate that vesicular drug accumulation is not important to DOX resistance in Dx5 cells. Furthermore, these studies demonstrate that altered endomembrane pH regulation is not a necessary consequence of cell transformation, and that vesicular sequestration of drugs is not a necessary characteristic of MDR.

MATERIALS AND METHODS

Cell lines

MES-SA human uterine sarcoma cells (Harker et al., 1983) and a multidrug-resistant derivative cell line (Dx5) (Harker and Sikic, 1985), were obtained from American Type Culture Collection (Manassas, VA). Cells were grown in McCoy's 5A medium with 1.5 mM L-glutamine supplemented with 10% fetal bovine serum, but no added antibiotics in order to ensure comparability between the two cell lines. Cells were passed every 3 to 4 days and growth medium changed daily. New cultures of cells were thawed every 2–3 weeks to prevent loss of the MDR phenotype by the Dx5 cells in culture. For fluorescence experiments, cells were plated four days prior to experiments on the coverslip of 35 mm coverslip-bottomed dishes (Mattek, Ashland, MA).

Proteins and chemicals

Human transferrin (Tf) was obtained from Sigma Chemical Co. (St. Louis, MO), iron loaded and purified by S300 column purification as described elsewhere (Yamashiro et al., 1984). Cyanine 5.18 succinimidyl ester (Cy5) was obtained from Amersham Co. (Arlington Heights, IL). All other fluorescent probes and amino dextran were obtained from Molecular Probes (Eugene, OR). All other reagents were obtained from Sigma Chemical Co. Fluorescent conjugates of Tf, horseradish peroxidase (HRP) and dextran were prepared from succinimidyl esters of various fluorophores according to manufacturer's instructions. For pH-sensitive dyes, transferrin was conjugated to both fluorescein and rhodamine (F-R-Tf) in a ratio of 6:2:1 and dextran was conjugated to fluorescein and rhodamine (F-R-dex) in a ratio of 4:4:1 (Dunn et al., 1994b).

Cell toxicity assay

Cells were seeded into 96 well plates at a density of 8000 per well, and grown for 24 h. Cells were then moved into growth medium containing 0, 3 10, 50, 500, 1000 and 10,000 nM DOX, with or without 6 μM verapamil, in which they were then grown for another 72 h.

Doxorubicin toxicity was assayed using the MTT assay, as previously described (Gosland et al., 1989; Gosland et al., 1996). The medium of each well was replaced with fresh medium containing 0.45 mg/ml of MTT (Sigma Chemical Co.), and incubated for 6 h. The dye solution was then removed and 100 μl of 0.1N analytical grade HCl (Fisher Scientific Corp., Chicago, IL) in 2-propanol (Sigma Chemical Co.) added to each well. Within 30 min the absorbance of each well was read on a Molecular Device SpectraMax 340 (Molecular Devices Corp., Sunnyvale, CA) plate reader, using a test wavelength of 570 nm, and a reference wavelength of 630 nm. Each condition was assayed in 16 replicate samples. IC 50 values were calculated from semi-logarithmic plots of the resulting values.

Fluorescence labeling of cells

Cells were labeled with fluorescent drugs by incubation in 2 μg/ml DOX or DNR in growth medium in a humidified 5% CO_2 atmosphere for 2 h prior to imaging. Specificity of DOX fluorescence was established from comparisons with unlabeled cells (which showed no lysosomal fluorescence) and cells labeled for 1 h (which showed reduced lysosomal fluorescence). Lysosomes were labeled by incubating cells overnight in either 20 μg/ml Cy5-HRP or Cy5-dextran, or for lysosome pH measurements, in 100 μg/ml F-R-dextran in growth medium in a humidified 5% CO_2 atmosphere. The cells were then rinsed and incubated for another 1.5 to 2.5 h to chase fluorescent probes through endosomes into lysosomes. The validity of specific labeling of lysosomes by extended incubations in fluid-phase probes has been previously established for both fluorescent dextrans (Ohkuma and Poole, 1978; Swanson, 1989) and HRP (Ward et al., 1997; Futter et al., 1998) and similar distributions were found for both probes. Endosomes were labeled by incubating cells for 20 min in 20 μg/ml Cy5-Tf or for endosome pH measurements, in 20 μg/ml F-R-Tf. Cells were incubated either in serum-free growth medium in a 5% CO_2 incubator or in Medium 1 (150 mM NaCl, 20 mM HEPES, 1 mM $CaCl_2$, 5 mM KCl, 1 mM $MgCl_2$, 10 mM glucose pH 7.4) on a slide warmer in a humidified chamber. For comparisons of drug and Tf distributions, cells were imaged in the continued presence of extracellular labels. For lysosomal localizations, lysosome imaging was conducted in medium containing fluorescent drugs, but lacking lysosomal label except in the case of the methylamine treatment study shown in Figure 3, where imaging was conducted immediately following exchange into drug-free medium.

Microscopy

All microscopy was conducted with living cells in coverslip-bottomed dishes, incubated (as indicated) in HEPES-buffered medium 1 or in bicarbonate-buffered growth medium on the microscope stage. Temperature was maintained at 37°C by a Medical Systems Corp. PDMI-2 perfusion chamber (Greenvale, NY) and for studies of cells in bicarbonate-buffered medium, dishes were superfused with 5% CO_2. Most experiments were conducted using a Bio-Rad MRC-1024 laser scanning confocal attachment mounted on a Nikon Diaphot 200 inverted microscope using a Nikon 60X N.A. 1.4 or Nikon 100X N.A. 1.4 oil immersion objectives. Illumination was provided by a Krypton-Argon laser providing for fluorescence excitations at 488 nm, 568 nm and 647 nm. The system is equipped with 3 photomultiplier tube detectors, allowing collection of up to 3 images simultaneously. Fluorescein fluorescence was excited using 488 nm illumination and collected through a 522 nm bandpass filter. DOX and rhodamine fluorescence were excited using 568 nm illumination and collected using a 598 nm bandpass filter. Cy5 fluorescence was excited using 647 nm illumination and collected through a 680 nm bandpass filter. Images were typically collected by averaging 2–5 scans. Photomultiplier offsets were set such that background (determined with the lightpath to the stage blocked) were slightly positive to guarantee signal linearity with fluorescence. Whenever possible, signal saturation was avoided, and objects with saturated pixels were omitted from quantifications. For the methylamine treatment study shown in Figure 3, images were taken using a Princeton Instruments Pentamax CCD detector mounted on a Nikon Diaphot 300 inverted microscope.

Image processing for presentation

Image processing was conducted using Metamorph software (Universal Imaging, West Chester, PA). In order to minimize photobleaching and phototoxicity in living cells, all fields were imaged with minimal averaging. To compensate, all images were subsequently averaged spatially using a 3×3 low pass filter. Images shown in comparable figures were contrast stretched identically to enhance the visibility of dim structures, and specific care was taken never to enhance the contrast in such a way that dim objects were deleted from an image. Montages were assembled and annotated using Photoshop (Adobe, Mountain View, CA).

Fluorescence ratio quantifications of drug accumulation

In order to quantify the enrichment of DOX in lysosomes, ratios of the fluorescence of DOX in lysosomes to the diffuse fluorescence of the cytoplasmic region of the same cells were calculated. Cells were labeled with DOX and Cy5-HRP and imaged by confocal microscopy as described above. The Cy5-HRP image was used as a stencil to identify lysosomes; a 4×4 pixel region defined by a single vesicle labeled with Cy5-HRP was identified, and mean DOX fluorescence in the corresponding pixels of the DOX image were quantified. DOX fluorescence was quantified for several lysosomes in a particular cell, as was the mean diffuse DOX fluorescence in a 4×4 pixel cytoplasmic region away from the nucleus, lysosomes and vesicular DOX. A constant value, reflecting the image offset, was subtracted from each value, and the ratio of fluorescence of DOX in lysosomes to that in the adjacent cytoplasm was calculated. For each condition 30–48 lysosomes from 10–12 cells were quantified.

Fluorescence ratio quantifications of pH

Images used for quantification were background corrected by subtracting from each pixel the median intensity from the surrounding 32×32 neighborhood (Maxfield and Dunn, 1990). Distinction of individual endosomes was conducted through an automated method that sequentially erodes pixels from an object (defined as a contiguous set of non-zero pixels) if the intensity of those pixels is below some fraction of the maximum pixel in the same object (Maxfield and Dunn, 1990). For endosome fluorescence ratio calculations, the common non-zero pixels for each endosome were determined and the fluorescence ratio within that region calculated. As much as possible, detector saturation was avoided during collection, but when pixel saturation occurred, objects with pixels within 10% of saturation (with a gray level of 230 or above in the original image) were removed from analysis. The methods used here are as described previously (Johnson et al., 1993; Dunn et al., 1994a; Dunn et al., 1994b; Dunn and Maxfield, 1998).

Endosome and lysosome acidification measurements were conducted using a fluorescence ratio technique described previously (Presley et al., 1993; Dunn et al., 1994b; van Weert et al., 1995; Presley et al., 1997; Dunn and Maxfield, 1998), which is based upon a procedure widely used by the laboratories of Murphy (e.g., Sipe et al. [1991]) and Verkman (e.g., Zen et al. [1992]).

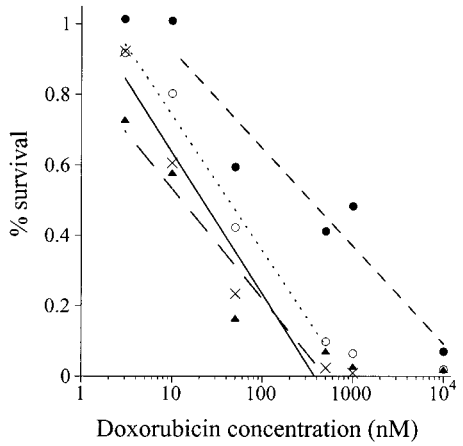

Fig. 1. Doxorubicin toxicity. Toxicity was assayed using the MTT assay, as described in Methods. Results are shown for Dx5 cells (closed circles), Dx5 cells in the presence of 6 μM verapamil (open circles), MES-SA cells (triangles) and MES-SA cells in the presence of 6 μM verapamil (crosses). Each point represents the mean of 14–16 samples.

Cells were incubated as described above with either F-R-Tf or F-R-dextran. For each vesicle the amount of fluorescein and rhodamine fluorescence was quantified, and the ratio calculated by digital image analysis as described above. Estimates of pH were derived from calibration curves established from parallel samples of cells that were fixed after incubation and equilibrated with a range of pH buffers.

RESULTS

In agreement with previous studies (Gosland et al., 1993; Gosland et al., 1989; Harker et al., 1986; Lau et al., 1994), Figure 1 shows that Dx5 cells are approximately 26 times more resistant to DOX when compared with the parental MES-SA cells (I.C. 50 341 nM versus 13 nM). As previously reported (Harker et al., 1986; Gosland et al., 1989; Gosland et al., 1993; Gosland et al., 1996; Chen et al., 1997), DOX resistance of Dx5 cells is sensitive to verapamil (I.C. 50 decreased to 42 nM), consistent with the suggested role of PGP in these cells (Luckie et al., 1996; Chen et al., 1997). Similar to previous studies (Lau et al., 1994; Dumontet et al., 1998), the reduced drug sensitivity of the Dx5 cells is correlated with reduced cellular accumulation, with a 2-h incubation in 2 μg/ml DOX resulting in nuclear labeling in 95% of MES-SA cells, but only 16% of Dx5 cells.

The studies described here take advantage of the intrinsic fluorescence of the drugs DOX and DNR to characterize the process of vesicular drug accumulation by confocal microscopy. All studies resulted from analysis of living cells, as the cellular localization of drugs has been found to depend upon active cellular metabolism ([Willingham et al., 1986] and see below). Furthermore, in order to characterize steady-state intracellular DOX distributions despite ongoing efflux mechanisms, imaging was conducted in the continuous presence of extracellular DOX. The ability of confocal microscopy to eliminate the out-of-focus fluorescence emanating from extracellular DOX made it possible to

collect high-resolution images of intracellular DOX without the fluorescence background that would have made imaging impossible by wide-field microscopy.

The fluorescent fluid-phase probes, Cy5-HRP, and Cy5-dextran were used to vitally label lysosomes. The validity of specific labeling of lysosomes by extended incubations in fluid-phase probes has been previously established for both fluorescent dextrans (Ohkuma and Poole, 1978; Swanson, 1989) and HRP (Ward et al., 1997; Futter et al., 1998) and similar results were found with either probe. Cy5 conjugates of these probes were chosen because their fluorescence emissions can be distinguished from that of DOX in the same cells. In order to evaluate the lysosomal localization of DOX, lysosomes were labeled by incubating cells with 20 μg/ml Cy5-HRP or Cy5-dextran overnight. Cells were then rinsed and incubated for another 2.5 h to chase the fluid-phase probe through endosomes into lysosomes. 2 μg/ml DOX (or DNR) was included in the cellular medium for the final 2 h prior to and during confocal imaging.

The confocal micrographs of living MES-SA cells imaged in the presence of extracellular DOX shown in Figure 2 show that DOX is preponderantly localized in the nucleus of these cells (A), but that the vesicular distribution of DOX in the cytosol corresponds vesicle-for-vesicle with that of Cy5-HRP in lysosomes (B, the arrows should be used as landmarks, as they indicate a small fraction of the DOX vesicles colocalizing with the lysosomal marker). This colocalization is also apparent in the color representation of these fields shown in Figure 6A. In comparable experiments, DNR was also found in a strictly lysosomal distribution (data not shown). Treatment of cells with 10 μM verapamil had no effect on the lysosomal distribution of DOX (Fig. 2, C and D). Similar results were obtained with cells incubated in HEPES-buffered medium in air or in bicarbonate-buffered medium in CO_2 (not shown).

Incubation with DOX in the presence of the v-H^+ATPase inhibitor bafilomycin completely blocked lysosomal accumulation of DOX (Fig. 2, E and F), indicating that lysosomal accumulation depends upon acidification. The importance of vesicular acidification to DOX accumulation in SA cells is also indicated by its rapid efflux from vesicles upon addition of the weak base methylamine, a treatment that alkalinizes lysosomes virtually instantaneously (data not shown). Figure 3 shows the results of an experiment in which cells were incubated in 2 μg/ml doxorubicin for 2 h, rinsed free of drug and imaged immediately by wide-field microscopy at the indicated times after addition of 80 mM methylamine. The speed of efflux from lysosomes indicates that at neutral pH, deprotonated DOX rapidly fluxes across lysosomal membranes. No drug efflux was detected in parallel, untreated controls (data not shown).

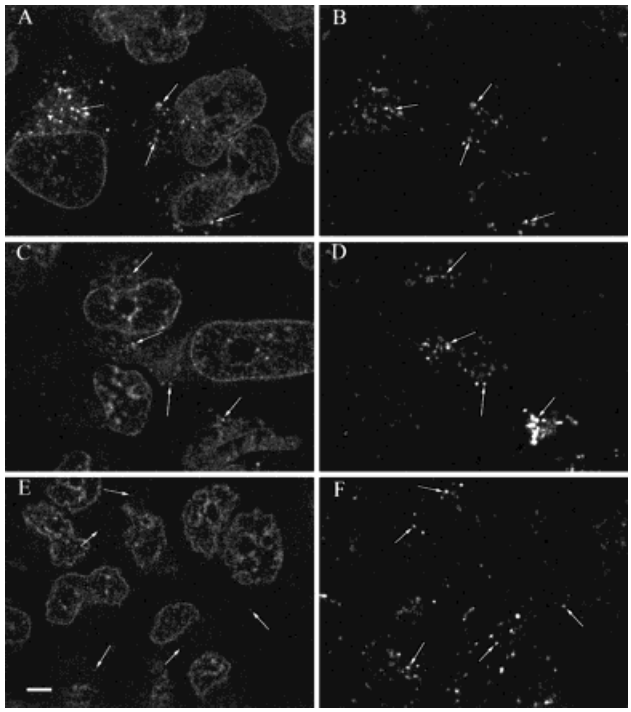

Fig. 2. Distribution of DOX (**left**) and Cy5-HRP (**right**) in living MES-SA cells. Cells were incubated with 20 μg/ml Cy5-HRP overnight, in medium alone for 30 min, then incubated for another 2 h in the presence of 2 μg/ml DOX alone (**A** and **B**), combined with 10 μM verapamil (**C** and **D**), or combined with 0.5 μM bafilomycin (**E** and **F**). Arrows indicate examples of lysosomes containing Cy5-HRP. Scale bar is 10 microns in length.

The confocal micrographs of living Dx5 cells imaged in the presence of extracellular DOX shown in Figure 4 show that, as expected, the overall cellular level of DOX was reduced in the resistant Dx5 cells. Verapamil treatment increased DOX labeling of both nucleus and

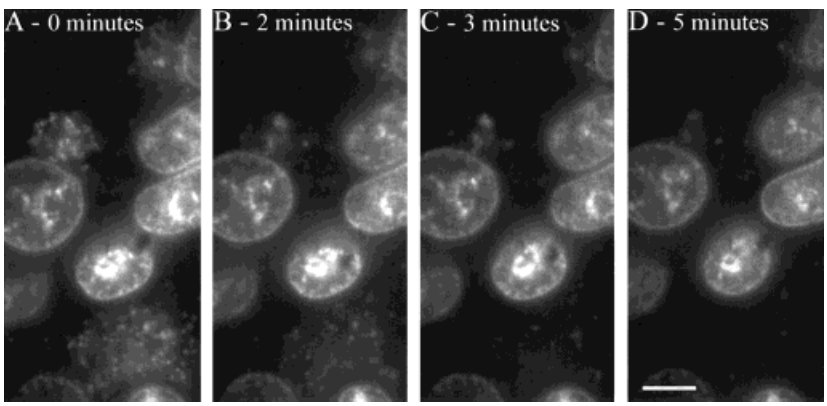

Fig. 3. Rapid efflux of DOX from lysosomes of MES-SA cells after treatment with methylamine. Cells were incubated in 2 μg/ml doxorubicin for two hours, rinsed free of drug and imaged immediately by wide-field microscopy at the indicated times after addition of 80 mM methylamine. No drug efflux was detected in parallel, untreated controls. Scale bar is 10 microns in length.

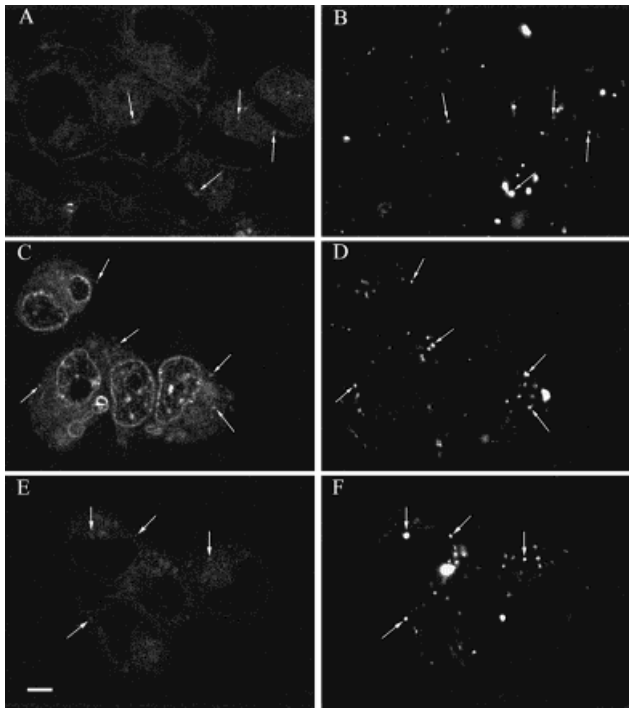

Fig. 4. Distribution of DOX (**left**) and Cy5-HRP (**right**) in living Dx5 cells. Cells were incubated with 20 μg/ml Cy5-HRP overnight, in medium alone for 30 min, then incubated for another 2 h in the presence of 2 μg/ml DOX alone (**A** and **B**), combined with 10 μM verapamil (**C** and **D**), or combined with 0.5 μM bafilomycin (**E** and **F**). Arrows indicate examples of lysosomes containing Cy5-HRP. Scale bar is 10 microns in length.

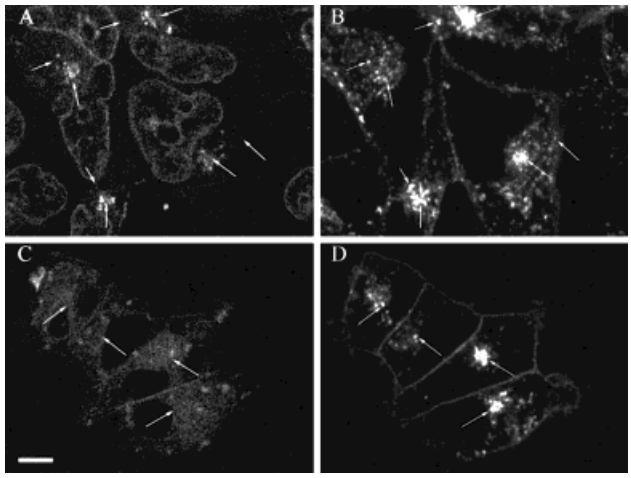

Fig. 5. Distribution of DOX and Cy5-Tf in living MES-SA (**A** and **B**) and Dx5 cells (**C** and **D**). Cells were incubated for 2 h in the presence of 2 μg/ml DOX, with 20 μg/ml Cy5-Tf included for the last 20 min. Arrows indicate examples of Tf-containing compartments that close comparison shows do not contain DOX. Scale bar is 10 microns in length.

cytoplasm of Dx5 cells (Figure 4C), consistent with previous results (Gosland et al., 1989; Chen et al., 1997) and with the suggested role of PGP in these cells (Luckie et al., 1996; Chen et al., 1997). Surprisingly however, vesicular DOX was found to be much less apparent in the PGP-expressing Dx5 cells. What little vesicular DOX was found in the Dx5 cells was localized to lysosomes as it colocalized closely with Cy5-HRP (Fig. 4B). DNR was likewise found in a lysosomal distribution in Dx5 cells (data not shown). Given the relatively small accumulation of DOX in lysosomes, the effects of verapamil and bafilomycin (Fig. 4, E and F) were difficult to discern. Similar results were obtained with cells incubated in HEPES-buffered medium in air or in bicarbonate-buffered medium in CO_2 (not shown).

In contrast to previous studies (Zamora and Beck, 1986; Sognier et al., 1994; Hurwitz et al., 1997), we see no evidence for elaboration of the lysosomal system. Indeed comparison of the number and HRP accumulation of lysosomes in Figures 2 and 4 indicate that the lysosome system is less pronounced in the resistant Dx-5 cells. Although this observation varied between experiments (for example note the similar lysosomal labeling of the two lines shown in Figure 6, C and D), the resistant Dx-5 cells were never observed to have a more extensive lysosomal system than the sensitive MES-SA cells.

Some studies have associated increased rates of membrane transport with MDR (Sehested et al., 1987a; Sehested et al., 1987b), or PGP (Warren et al., 1991). In order to determine whether the difference in the number or HRP-labeling of lysosomes between the two cell lines reflected differences in lysosomal exocytosis, the lysosomal labeling of cells imaged immediately following incubation with fluorescent dextrans was compared with that of cells imaged after a 2-h chase. Little or no dextran efflux was detected in either cell line, indicating that the large difference in vesicular drug accumulation found between MES-SA and Dx5 cells could not be attributed to different rates of lysosomal exocytosis in the two cell lines (data not shown).

Recent evidence suggests that PGP may be internalized into endosomes from which it is recycled to the plasma membrane (Kim et al., 1997). To evaluate the question of whether DOX is present in endosomes of the recycling pathway, the distribution of DOX was compared with that of the endocytic probe, Cy5-Tf in living cells. Tf remains bound to its receptor throughout its endocytic itinerary, making it an excellent vital marker of the recycling endocytic pathway (Dunn et al., 1989). As with the above studies comparing the distribution of DOX with lysosomes, Cy5-Tf was chosen since its fluorescence emissions can be distinguished from, and thus compared with that of, DOX in the same living cells. Cells were incubated for 2 h in the presence of 2 μg/ml DOX, with 20 μg/ml Cy5-Tf included for the last 20 min prior to imaging live in the presence of both DOX and Cy5-Tf.

Figure 5 shows that although vesicular DOX and Tf both occur in the same perinuclear location, the two probes do not colocalize in the same vesicles in either cell line. Using the arrows in this figure to indicate vesicles containing DOX, careful examination of 5A and 5B shows clear differences in the vesicular patterns of DOX and Tf fluorescence, with the two probes frequently labeling adjacent vesicles in the MES-SA cells. These differences are more obvious in the color representation of this image shown in Figure 6B, which shows that the patterns of the two probes are distinctly

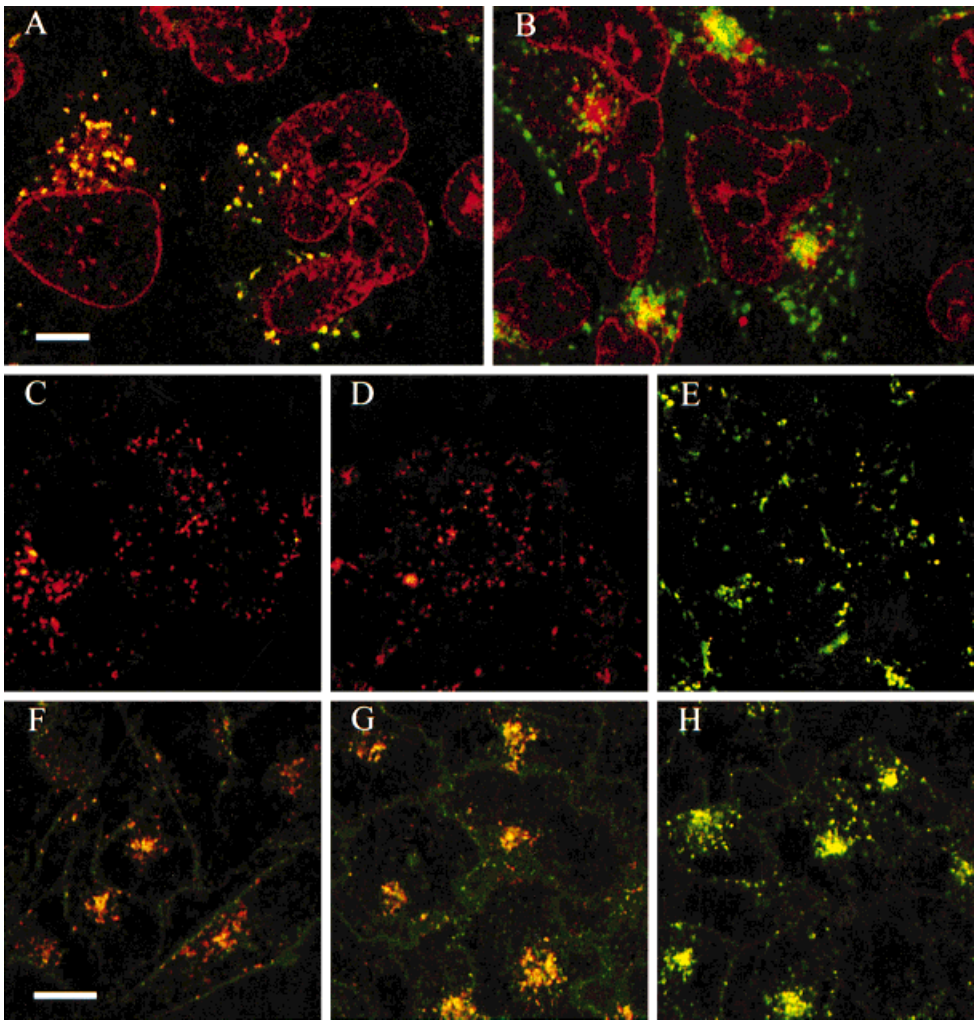

Fig. 6. Distribution of DOX and Cy5-HRP in living MES-SA cells (**A**) and living MES-SA cells (**B**). Cells were treated as described in Figure 1. Fluorescence of pH-sensitive F-R-dextran in living MES-SA cells (**C**), MES-SA/Dx5 cells (**D**) and MES-SA/Dx5 cells (**E**) 27 min after treatment with 0.5 μM bafilomycin. Cells were incubated in 100 μg/ml F-R-dextran overnight, then chased in the absence of dextran for 2 h prior to imaging. Fluorescence of pH-sensitive F-R-transferrin in living MES-SA cells (**F**), MES-SA/Dx5 cells (**G**) and MES-SA/Dx5 cells (**H**) 5 minutes after treatment with 0.5 μM bafilomycin. Cells were incubated in 20 μg/ml F-R-Tf for 20 min prior to and during imaging. Scale bars are 10 microns in length, with bar in A pertaining to panels A–E and bar in F pertaining to F–H.

different, in striking contrast to the colocalization of DOX with lysosomal Cy5-HRP shown in Figure 6A. Similar results were found in studies of the Dx5 cells, which showed no overlap in the vesicular distribution of DOX (Fig. 5C) and Tf (Fig. 5D). Although these studies do not preclude the possibility that low levels of DOX in endosomes were not detected in these studies, they demonstrate that the accumulation of DOX in endosomes is minimal relative to that in lysosomes. MES-SA and Dx5 cells showed similar levels of steady-state Tf labeling but, as in previous studies, MES-SA cells displayed significantly more vesicular DOX labeling.

Our observation that drug-resistant Dx5 cells manifest less vesicular DOX than the parental MES-SA cells contrasts with many previous studies that associate vesicular drug accumulations with activity of PGP (Gervasoni et al., 1991; Sognier et al., 1992; Sognier et al., 1994; Seidel et al., 1995; Cleary et al., 1997), or MRP (Gervasoni et al., 1991; Breuninger et al., 1995). We considered two possible explanations for why vesicular DOX accumulation might be less prominent in the PGP-expressing Dx5 cell line. The first possibility is that the level of cytosolic DOX is minimal in Dx5 cells by virtue of exclusion of DOX from the cytosol, due either to the pumping activity of PGP at the plasma membrane, or to PGP-dependent differences in cytosolic pH (Keizer and Joenje, 1989; Boscoboinik et al., 1990; Thiebaut et al., 1990; Roepe, 1992; Luz et al., 1994; Simon et al., 1994; Altan et al., 1998). The second possibility is that the pH gradient required for lysosomal DOX accumulation is not present in the Dx5 cells. These possibilities were analyzed as described below.

The images shown in Figures 2 and 4 argue against the possibility that lower levels of vesicular DOX in Dx5 cells result from lower levels of cytosolic DOX, as cytosolic DOX fluorescence is relatively strong in Dx5 cells, particularly following treatment with verapamil.

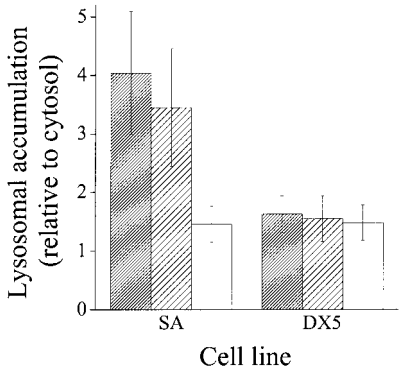

Fig. 7. Lysosomal accumulation of doxorubicin in MES-SA and Dx-5 cells. As described in Methods, lysosomal accumulation of DOX was quantified for cells incubated with 20 μg/ml Cy5-HRP overnight, in medium alone for 30 min, then incubated for another 2 h in the presence of 2 μg/ml DOX alone (solid bars), combined with 10 μM verapamil (hatched bars), or combined with 0.5 μM bafilomycin (open bars). Bars indicate the fluorescence of DOX in lysosomes relative to that in the cytosol. For each sample, 30–48 lysosomes from 10–12 cells were analyzed. Error bars indicate standard deviations.

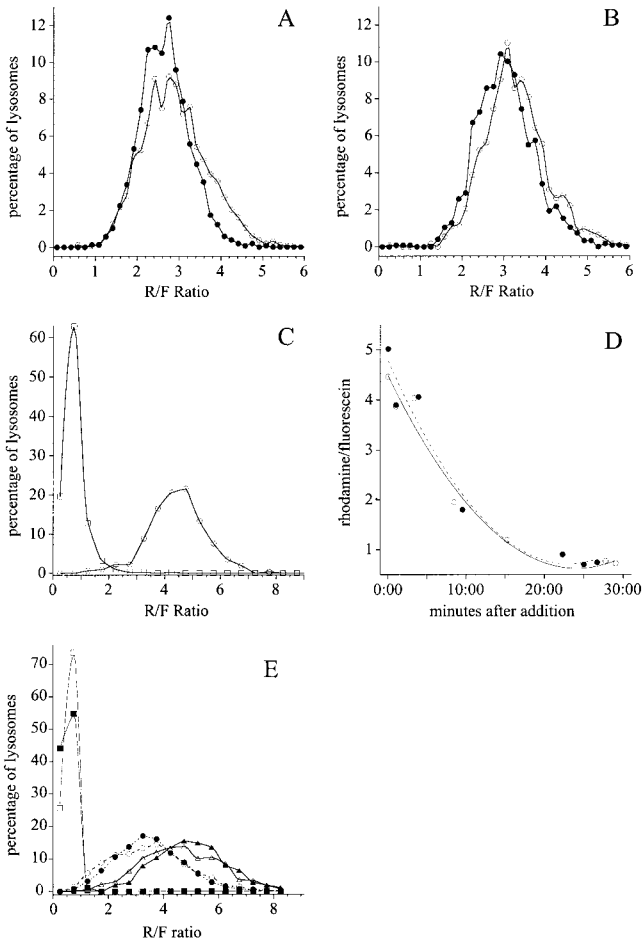

Fig. 8. Frequency histograms of rhodamine/fluorescein emission ratios of F-R-dextran-labeled lysosomes in living cells. Cells were incubated in 100 μg/ml F-R-dextran overnight, then chased in the absence of dextran for 2 h prior to imaging in bicarbonate buffered growth medium in 5% CO_2 (**A**) or HEPES-buffered Medium 1 in air (**B**). Open circles - MES-SA cells (N = 1627 in A, 1261 in B). Closed circles - Dx5 cells (N = 1564 in A, 1261 in B). **C:** Effect of bafilomycin on lysosome pH. Data are shown for MES-SA cells before (circles, N = 316) and 28 min after treatment with 0.5 μM bafilomycin (squares, N = 409). **D:** Time series of median rhodamine/fluorescein emission ratios of F-R-dextran-labeled lysosomes in living MES-SA cells (open circles), and MES-SA/Dx5 cells (closed circles) following addition of 0.5 μM bafilomycin. Sample sizes ranged from 70–240 lysosomes for each time point. **E:** Effects of verapamil and bafilomycin on rhodamine/fluorescein emission ratios of F-R-dextran-labeled lysosomes in living cells. Cells were incubated in 100 μg/ml F-R-dextran overnight, then chased in the absence of dextran for 2 h in the presence of 0.5 μM bafilomycin (open squares - MES-SA cells, N = 1700, closed squares - Dx5 cells, N = 1694), 10 μM verapamil (open circles - MES-SA cells, N = 1577, closed circles - Dx5cells, N = 1429), or 0.1% ethanol (equivalent to the volume used as carrier for verapamil-treatment) (open triangles - MES-SA cells, N = 938, closed triangles - Dx5 cells, N = 635).

Comparisons with control cells verified that the cytosolic fluorescence in these images derives from DOX, rather than from autofluorescence. To circumvent cell–cell differences in cytosolic levels of DOX, we quantified the fluorescence of DOX in lysosomes relative to that in the cytosol. The intensities of DOX fluorescence in lysosomes (identified by Cy5-HRP labeling) were compared with that in the immediate adjacent cytoplasm of the same cells (see Methods and Materials). The results of this analysis are shown in Figure 7. The sensitive MES-SA cells showed a four-fold increased DOX fluorescence in lysosomes over that in the cytosol, which was largely insensitive to verapamil, but was nearly completely blocked by bafilomycin. In contrast, we measured minimal accumulation of DOX in the lysosomes of the resistant Dx5 cells under any condition. Taken together, these results argue that the reduced lysosomal accumulation of DOX seen in Dx5 cells does not result from lower levels of cytosolic DOX. One should note that because of potential environmental effects on DOX fluorescence, these quantifications are not intended to provide absolute estimates of DOX accumulation in lysosomes.

The dramatic effects of bafilomycin and methylamine on lysosomal accumulation of DOX in MES-SA cells indicates that lysosomal acidification is critically important to DOX accumulation in lysosomes. In order to determine whether the lower level of vesicular drug accumulation found in the resistant Dx5 cells resulted from faulty lysosomal acidification, we directly measured the pH of individual lysosomes. Lysosomes were labeled by overnight incubation of cells with a pH-sensitive form of dextran conjugated to both fluorescein and rhodamine. As has been shown previously, the ratio of the fluorescence of fluorescein (which is pH sensitive) to rhodamine (which is not) is a sensitive indicator of pH (Johnson et al., 1993; Presley et al., 1993; Dunn et al., 1994a; Dunn et al., 1994b; van Weert et al., 1995; Presley et al., 1997; Dunn and Maxfield, 1998). Cells were incubated in 100 μg/ml F-R-dextran overnight, then chased in the absence of dextran for 2 h prior to imaging live by confocal microscopy. Images of representative fields of living MES-SA and Dx5 cells are shown in Figure 6C and 6D, respectively. At the acidic pH of lysosomes, fluorescein fluorescence is effectively quenched, leaving the F-R-dextran in lysosomes fluorescing red. The alkalinizing effect of bafilomycin is apparent in the green fluorescence of the lysosomes of Dx5 cells shown in 6E, reflecting the in-

creased fluorescein fluorescence that accompanies lysosome alkalization. Bafilomycin treatment had an identical effect on lysosome fluorescence of MES-SA cells (not shown, see below).

Quantifications of these images indicate that the differences in DOX accumulation do not derive from differences in lysosomal acidification between MES-SA and Dx5 cells. Histograms of the R/F ratios of F-R-dextran-labeled lysosomes are shown in Figure 8. The two cell lines showed similar R/F ratios for cells maintained either in a bicarbonate-buffered medium in 5% CO_2 (Figure 8A), or in HEPES-buffered Medium 1 in air (Figure 8B). The R/F ratios of untreated cells indicate a similar lysosome pH in the two cell lines, with the median ratio indicating a pH < 4.5, the lower limit we were able to quantify in our fixed calibration samples. Measurements of cells treated with bafilomycin indicate that inhibiting the v-ATPase alkalinizes the lysosomes of both cell lines to a pH of 6.8. The effect of bafilomycin on lysosome R/F ratios of MES-SA cells is shown in Figure 8C. Figure 8D shows that lysosome alkalization occurs with identical kinetics in the two cell lines. Taken together, these studies indicate that that development of multidrug-resistance and the expression of PGP by the Dx5 cells has no effect on either steady-state lysosome pH nor on the dynamics of proton transport in lysosomes.

Interestingly, the differences in lysosomal DOX accumulation shown in Figure 7 correspond to differences in lysosomal pH in the MES-SA cells, but not in the Dx5 cells. For comparability with the conditions used in the lysosomal accumulation studies, cells were treated with bafilomycin, verapamil or equivalent volumes of carriers for 2 h, and the pH of lysosomes measured. The results of this analysis are shown in Figure 8E. The bafilomycin treatment that blocked lysosomal accumulation of DOX in MES-SA cells, completely alkalinized lysosomes of both cell lines (to a pH of 7.2–7.3). The verapamil treatment that modestly decreased lysosomal DOX accumulation in MES-SA cells, modestly increased lysosome pH in both cell lines from below 4.5 to 4.6–4.7. However, this relationship does not hold for Dx5 cells, in which lysosomal DOX accumulation was minimal regardless of lysosome pH.

Given the recent evidence that PGP is present in recycling endosomes (Kim et al., 1997), we conducted experiments to establish the potential role of PGP in regulating endosome pH using F-R-Tf as a pH-sensitive probe of the recycling pathway. As discussed above, the presence of PGP might be expected to enhance acidification of endomembrane compartments through its Cl^- channel activity. Cells were incubated in 20 μg/ml F-R-Tf for 20 min prior to confocal imaging, and then imaged in the continued presence of extracellular F-R-Tf. Images of representative fields of living MES-SA and Dx5 cells are shown in Figure 6F and 6G, respectively. The fluorescence of the ligand derives from both fluorescein and rhodamine so that endosomes appear yellow, due to the quenching of fluorescein's fluorescence at the acidic pH of endosomes, while ligand bound to the plasma membrane (awaiting internalization) appears green, due to the strong fluorescence of fluorescein at neutral pH. A field of Dx5 cells imaged 5 min after addition of bafilomycin is shown in 6H.

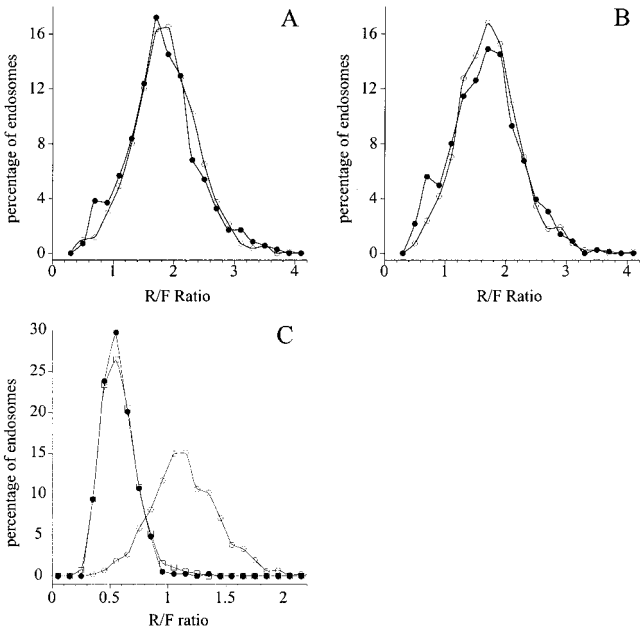

Fig. 9. Frequency histograms of rhodamine/fluorescein emission ratios of F-R-Tf-labeled endosomes in living cells. Cells were incubated for 20 min and then imaged in 20 μg/ml in F-R-Tf in either bicarbonate-buffered growth medium in 5% CO_2 (**A**) or HEPES-buffered Medium 1 in air (**B**). Open circles - MES-SA cells (N = 1120 in A, 839 in B). Closed circles - Dx5 cells (N = 703 in A, 785 in B). **C:** Effect of bafilomycin and methylamine on endosome pH of MES-SA cells. Data are shown for MES-SA cells before (open circles, N = 874) and 5–10 minutes after treatment with 0.5 μM bafilomycin (squares, N = 963) or 40 mM Methylamine (closed circles, N = 373).

Images collected in this way were quantified by digital image analysis, and the resulting R/F ratios are shown in Figure 9. These analyses showed very similar pH in the recycling endosomes of either MES-SA and Dx5 cells, regardless of whether cells were incubated in a bicarbonate-buffered medium in 5% CO_2 (Figure 9A) or in HEPES-buffered Medium 1 in air (Figure 9B). The pH of recycling endosomes was calculated to be 5.8 for the MES-SA cells and 5.9 for the Dx5 cells, values similar to previous studies of fibroblasts (Yamashiro et al., 1984; Johnson et al., 1993; Presley et al., 1993). It is clear that the potential presence of PGP in endosomes of the recycling pathway does not enhance endosome acidification. This conclusion is also supported by experiments that showed verapamil has no effect on endosome pH (data not shown). As expected, bafilomycin treatment raised the pH of recycling endosomes of Dx5 and MES-SA cells to 7.0 and 6.9, respectively (Figure 9C).

DISCUSSION

The literature on the nature and role of intracellular vesicles in MDR is highly variable and frequently contradictory (Simon and Schindler 1994), a situation that probably reflects the phenotypic diversity of MDR, even within the context of cells expressing PGP. We have addressed the relationship between multidrug-resistance, vesicular acidification and vesicular drug accumulation in the MES-SA human uterine sarcoma cell line (Harker et al., 1983) and the Dx5 derivative cell

line (Harker and Sikic, 1985). The Dx5 cells have repeatedly demonstrated multidrug-resistance (Harker et al., 1986; Gosland et al., 1993; Lau et al., 1994; Gosland et al., 1996; Chen et al., 1997; Dumontet et al., 1998), and express PGP (Gosland et al., 1989; Luckie et al., 1996; Chen et al., 1997), but not MRP (Chen et al., 1997). We find that MES-SA and Dx5 cells manifest the same properties of cellular drug accumulation and sensitivity as previously described, but differ from previously described models of MDR in several important respects. Even to the extent that these differences are unusual in the spectrum of cellular manifestations of MDR, they have important implications for understanding the mechanisms of MDR.

Taking advantage of the intrinsic fluorescence of DOX, studies were conducted to characterize the vesicular accumulation of drugs in living MES-SA and Dx5 cells by confocal microscopy. These studies show that nuclear accumulation of DOX is reduced in the Dx5 drug-resistant cell line in a verapamil-sensitive manner, consistent with PGP-mediated drug resistance. However, while many previous studies have associated MDR with vesicular accumulation of drugs (Gervasoni et al., 1991; Sognier et al., 1992; Sognier et al., 1994; Breuninger et al., 1995; Seidel et al., 1995; Cleary et al., 1997; Altan et al., 1998; Shapiro et al., 1998), we find that vesicular drug accumulation is more pronounced in the sensitive MES-SA cells than in the DOX-resistant Dx5 cells. Although other studies have shown vesicular drug accumulation in sensitive as well as resistant cells (Willingham et al., 1986; Lautier et al., 1997), this is the first study to our knowledge that describes a system in which MDR cells exhibit minimal vesicular drug accumulations.

Previous studies have indicated that drugs accumulate in Golgi-derived vesicles (Klohs and Steinkampf, 1988; Lautier et al., 1997; Altan et al., 1998), endosomes (Altan et al., 1998) and lysosomes (Warren et al., 1991; Hurwitz et al., 1997; Altan et al., 1998). Many of these studies compared the distribution of fluorescent drugs to organelle markers in separate cells, or in sequentially-labeled cells. Our characterizations of living cells simultaneously labeled with multiple probes allowed comparison of the distribution of drugs and fluorescent endosome and lysosome markers within the same cells. The importance of simultaneous comparisons within the same cells is emphasized by our comparisons of the vesicular distributions of DOX and endosomal transferrin, which appear very similar, but can be clearly distinguished by close comparison. Our studies unequivocally demonstrate that in both MES-SA and Dx5 cells, DOX and DNR accumulate predominately in lysosomes, as they showed a vesicle-for-vesicle correspondence between the fluorescent drugs and fluid-phase probes that had been chased into lysosomes.

MDR has also been associated with various alterations in the endocytic apparatus, some of which have been suggested to be important to drug transport (Beck, 1987; Simon and Schindler, 1994). Many MDR cells are characterized by an elaboration of the endosome/lysosome system (Zamora and Beck, 1986; Sognier et al., 1994; Hurwitz et al., 1997), which has been suggested to increase the volume of the compartment available for drug sequestration and/or secretion. However, we find no evidence for an increased number or volume of endocytic or lysosomal elements in resistant Dx5 cells. Increased rates of membrane transport have been associated with MDR (Sehested et al., 1987a; Sehested et al., 1987b), and with PGP (Warren et al., 1991), and interpreted in terms of enhancing vesicular drug transport in MDR cells. Altered membrane transport may also be indicated by the observation that the endocytic recycling compartment of MCF-7 tumor cells is disrupted, but intact in the adriamycin-resistant subclone (Schindler et al., 1996; Altan et al., 1998). In contrast, the endocytic recycling compartment is intact in both MES-SA and Dx5 cells and pulse-chase experiments indicate no difference in rates of lysosomal efflux between Dx5 and MES-SA cells (data not shown).

Several results indicate that vesicular drug accumulation is driven by vesicle transmembrane pH gradients. In both MES-SA and Dx5 cells, DOX and DNR were found to label lysosomes, whose pH was measured as < 4.5, but not recycling endosomes, whose pH was measured as 5.8–5.9. Not only were these weakly basic drugs associated with lysosomes, the most acidic organelle, but lysosomal accumulation of DOX by MES-SA cells was found to be completely sensitive to treatment with the v-H^+ATPase inhibitor, bafilomycin and to the weak-base methylamine, both of which were found to alkalinize lysosomes. The rapid loss of DOX from lysosomes upon addition of methylamine demonstrates that lysosomal accumulation is inhibited by the disruption of the lysosomal pH gradient, rather than by decreased whole-cell uptake of DOX. While the degree of lysosomal accumulation correlated well with lysosome pH for the MES-SA cells, vesicular accumulation of DOX was minimal in the Dx5 cells despite lysosomal pH values that were nearly identical to those of the MES-SA cells. The pH of recycling endosomes was also identical in the two cell lines. These results contrast with several previous studies, which have found defective endosome and lysosome acidification in tumor cell lines (Schindler et al., 1996; Millot et al., 1997; Altan et al., 1998).

The minimal lysosomal accumulation of DOX by Dx5 cells might reflect low cytosolic drug levels due to efficient exclusion at the plasma membrane. However, the observation that lysosomal accumulation was minimal even when cellular levels of DOX were increased by verapamil treatment is surprising. These data suggest that anthracycline drugs may not be freely diffusible in the cytosol of Dx5 cells. Further studies are required to establish why Dx5 cells are refractory to vesicular drug accumulation.

Another possible explanation for the minimal lysosomal drug accumulation of Dx5 cells is that the pH gradient across the lysosome membranes of Dx5 cells is reduced due to an acidified cytosol. Insofar as an acidic cytosol reduces the transmembrane pH gradient of intracellular vesicles, it might be expected to inhibit vesicular accumulation of weakly basic drugs. However, it is unlikely that the decreased lysosomal accumulation found in Dx5 cells can be explained by variation in cytosolic pH. First, the range of cytosolic pH variation is small relative to the pH gradient between the cytosol and lysosomes. Second, Simon et al. (1994) found that vesicular accumulation of daunomycin was reduced by alkalinizing rather than acidifying the cytosol. As cy-

tosol alkalization also decreased cellular drug accumulation in that study, it seems likely that cytosolic alkalization affects vesicular accumulation only indirectly, decreasing cytosolic levels of drug by decreasing the size the pH gradient across the plasma membrane. Indeed it has been suggested that much of the characteristic drug transport of MDR can be explained by the pH gradient across the plasma membrane (Simon and Schindler, 1994; Wadkins and Roepe, 1997), a question beyond the scope of this study.

Within the context of the phenotypic variability of MDR it is not possible to derive global conclusions about the role of vesicular drug accumulation in MDR from our studies of MES-SA and Dx5 cells. Although it has been established that the multi-drug resistance of Dx5 cells is correlated with the expression of PGP (Gosland et al., 1989; Luckie et al., 1996; Chen et al., 1997), but not MRP (Chen et al., 1997), it is possible that other transporters or characteristics of the Dx5 cells may participate in its drug resistance. In the spectrum of MDR phenotypes, Dx5 cells appear to be unusual in their lack of vesicular drug accumulation. Indeed, the Dx5 cells are especially unusual in that they are refractory to the accumulation of weakly basic drugs in lysosomes despite the presence of transmembrane pH gradients capable of concentrating drugs in the parental MES-SA cell line. In any case, our data indicate that accumulation of drugs like DOX and DNR in intracellular vesicles is not important to the MDR phenotype in the MES-SA/Dx5 cell system, and therefore is not necessarily important to MDR in all cell systems.

The MES-SA/Dx5 cell system provides a valuable exception to the PSS model (Schindler et al., 1996; Altan et al., 1998), which suggests multi-drug resistance is accomplished through the rescue of defective mechanisms of pH regulation, vesicular sequestration, and secretion found in transformed cell lines. While this model provides an attractive explanation for MDR for many experimental systems, the MES-SA/Dx5 cell system demonstrates that altered endomembrane pH regulation is not a necessary consequence of cell transformation, and that vesicular sequestration of drugs is not a necessary characteristic of MDR. These results emphasize the generic character of MDR as a phenotypically variable process that likely results from multiple mechanisms.

ACKNOWLEDGMENTS

This work was supported by grant #IRG-161-K from the American Cancer Society (KD), N.I.H. grant R29DK51098 (KD) and a fellowship from the American Heart Association, Indiana Affiliate, Inc. (EW).

LITERATURE CITED

Altan N, Chen Y, Schindler M, Simon SM. 1998. Defective acidification in human breast tumor cells and implications for chemotherapy. J Exp Med 187:1583–1598.

BaeHR, Verkman AS. 1990. Protein kinase A regulates chloride conductance in endocytic vesicles from proximal tubule. Nature 348: 637–639.

Barasch J, Gershon MD, Nunez EA, Tamir H, al-Awqati Q. 1988. Thyrotropin induces the acidification of the secretory granules of parafollicular cells by increasing the chloride conductance of the granular membrane. J Cell Biol 107:2137–2147.

Beck WT. 1987. The cell biology of multiple drug resistance. Biochem Pharmacol 36:2879–2887.

Boscoboinik D, Gupta RS, Epand RM. 1990. Investigation of the relationship between altered intracellular pH and multidrug resistance in mammalian cells. Br J Cancer 61:568–572.

BreuningerLM, Paul S, Gaughan K, Miki T, Chan A, Aaronson SA, Kruh GD. 1995. Expression of multidrug resistance-associated protein in NIH/3T3 cells confers multidrug resistance associated with increased drug efflux and altered intracellular drug distribution. Cancer Res 55:5342–5347.

Chen G, Duran GE, Steger KA, Lacayo NJ, Jaffrezou JP, Dumontet C, Sikic BI. 1997. Multidrug-resistant human sarcoma cells with a mutant P-glycoprotein, altered phenotype, and resistance to cyclosporins. J Biol Chem 272:5974–5982.

Cleary I, Doherty G, Moran E, Clynes M. 1997. The multidrug-resistant human lung tumour cell line, DLKP-A10, expresses novel drug accumulation and sequestration systems. Biochem Pharmacol 53: 1493–1502.

Cole SP, Bhardwaj G, Gerlach JH, Mackie JE, Grant CE, Almquist KC, Stewart AJ, Kurz EU, Duncan AM, Deeley RG. 1992. Overexpression of a transporter gene in a multidrug-resistant human lung cancer cell line [see comments]. Science 258:1650–1654.

de Lange JH, Schipper NW, Schuurhuis GJ, ten Kate TK, van Heijningen TH, Pinedo HM, Lankelma J, Baak JP. 1992. Quantification by laser scan microscopy of intracellular doxorubicin distribution. Cytometry 13:571–576.

Dumontet C, Bodinf, Michal y. 1998. Potential interactions between antitubulin agents and temperature: implications for modulation of multidrug resistance. Clin Cancer Res 4:1563–1566.

Dunn K, Maxfield FR. 1998. Ratio imaging instrumentation. Methods Cell Biol 56:217–236.

Dunn KW, Mayor S, Myers JN, Maxfield FR. 1994a. Applications of ratio fluorescence microscopy in the study of cell physiology. FASEB J 8:573–582.

Dunn KW, McGraw TE, Maxfield FR. 1989. Iterative fractionation of recycling receptors from lysosomally destined ligands in an early sorting endosome. J Cell Biol 109:3303–3314.

Dunn KW, Park J, Semrad CE, Gelman DL, Shevell T, McGraw TE. 1994b. Regulation of endocytic trafficking and acidification are independent of the cystic fibrosis transmembrane regulator. J Biol Chem 269:5336–5345.

Endicott JA, Ling V. 1989. The biochemistry of P-glycoprotein-mediated multidrug resistance. Ann Rev Biochem 58:137–171.

Fuchs R, Male P, Mellman I. 1989. Acidification and ion permeabilities of highly purified rat liver endosomes. J Biol Chem 264:2212–2220.

Futter CE, Gibson A, Allchin EH, Maxwell S, Ruddock LJ, Odorizzi G, Domingo D, Trowbridge IS, Hopkins CS. 1998. In polarized MDCK cells basolateral vesicles arise from clathrin-gamma-adaptin-coated domains on endosomal tubules. J Cell Biol 141:611–623.

Gervasoni Jr JE, Fields SZ, Krishna S, Baker MA, Rosado M, Thuraisamy K, Hindenburg AA, Taub RN. 1991. Subcellular distribution of daunorubicin in P-glycoprotein-positive and -negative drug-resistant cell lines using laser-assisted confocal microscopy. Cancer Res 51:4955–4963.

Gosland M, Tsuboi C, Hoffman T, Goodin S, Vore M. 1993. 17 beta-estradiol glucuronide: an inducer of cholestasis and a physiological substrate for the multidrug resistance transporter. Cancer Res 53:5382–5385.

Gosland MP., Gillespie MN, Tsuboi CP, Tofiq S, Olson JW, Crooks PA, Aziz SM. 1996. Reversal of doxorubicin, etoposide, vinblastine, and taxol resistance in multidrug resistant human sarcoma cells by a polymer of spermine. Cancer Chemother Pharmacol 37:593–600.

Gosland MP, Lum BL, Sikic BI. 1989. Reversal by cefoperazone of resistance to etoposide, doxorubicin, and vinblastine in multidrug resistant human sarcoma cells. Cancer Res 49:6901–6905.

Gottesman MM, Pastan I. 1993. Biochemistry of multidrug resistance mediated by the multidrug transporter. Ann Rev Biochem 62:385–427.

Harker WG, Bauer D, Etiz BB, Newman RA, Sikic BI. 1986. Verapamil-mediated sensitization of doxorubicin-selected pleiotropic resistance in human sarcoma cells: selectivity for drugs which produce DNA scission. Cancer Res 46:2369–2373.

Harker WG, MacKintosh FR, Sikic BI. 1983. Development and characterization of a human sarcoma cell line, MES-SA, sensitive to multiple drugs. Cancer Res 43:4943–4950.

Harker WG, Sikic BI. 1985. Multidrug (pleiotropic) resistance in doxorubicin-selected variants of the human sarcoma cell line MES-SA. Cancer Res 45:4091–4096.

Hoffman MM, Wei LY, Roepe PD. 1996. Are altered pHi and membrane potential in hu MDR 1 transfectants sufficient to cause MDR protein-mediated multidrug resistance? J General Physiol 108:295–313.

Hurwitz SJ, Terashima M, Mizunuma N, Slapak CA. 1997. Vesicular anthracycline accumulation in doxorubicin-selected U-937 cells: participation of lysosomes. Blood 89:3745–3754.

Johnson LS, Dunn KW, Pytowski B, McGraw TE. 1993. Endosome acidification and receptor trafficking: bafilomycin A1 slows receptor externalization by a mechanism involving the receptor's internalization motif. Mol Biol Cell 4:1251–1266.

Keizer HG, Joenje H. 1989. Increased cytosolic pH in multidrug-resistant human lung tumor cells: effect of verapamil. J Natl Cancer Inst 81:706–709.

KimH, Barroso M, Samanta R, Greenberger L, Sztul E. 1997. Experimentally induced changes in the endocytic traffic of P-glycoprotein alter drug resistance of cancer cells. Am J Physiol 273:C687–C702

Klohs WD, Steinkampf RW. 1988. The effect of lysosomotropic agents and secretory inhibitors on anthracycline retention and activity in multiple drug-resistant cells. Molecular Pharmacology 34:180–185.

Lau DH, Duran GE, Lewis AD, Sikic BI. 1994. Metabolic conversion of methoxymorpholinyl doxorubicin: from a DNA strand breaker to a DNA cross-linker. Br J Cancer 70:79–84.

Lautier D, Bailly JD, Demur C, Herbert JM, Bousquet C, Laurent G. 1997. Altered intracellular distribution of daunorubicin in immature acute myeloid leukemia cells. Int J Cancer 71:292–299.

Lelong IH, Guzikowski AP, Haugland RP, PastanI, Gottesman MM, Willingham MC. 1991. Fluorescent verapamil derivative for monitoring activity of the multidrug transporter. Mol Pharmacol 40: 490–494.

Luckie DB, Krouse ME, Law TC, Sikic BI, Wine JJ. 1996. Doxorubicin selection for MDR1/P-glycoprotein reduces swelling-activated K+ and Cl- currents in MES-SA cells. Am J Physiol 270:C1029–C1036

Luz JG, Wei LY, Basu S, Roepe PD. 1994. Transfection of mu MDR 1 inhibits Na(+)-independent Cl-/-HCO3 exchange in Chinese hamster ovary cells. Biochemistry 33:7239–7249.

Ma L, Center MS. 1992. The gene encoding vacuolar H(+)-ATPase subunit C is overexpressed in multidrug-resistant HL60 cells. Biochem Biophys Res Commun 182:675–681.

Marquardt D, Center MS. 1991. Involvement of vacuolar H(+)-adenosine triphosphatase activity in multidrug resistance in HL60 cells. J Natl Cancer Inst 83:1098–1102.

Maxfield FR, Dunn K. 1990. Studies of endocytosis using image identification fluorescence microscopy and digital image analysis. In: Herman B, Jacobson K, editors. Optical Microscopy for Biology. Wiley-Liss, Inc., 357–371.

Millot C, Millot JM, Morjani H, Desplaces A, Manfait M. 1997. Characterization of acidic vesicles in multidrug-resistant and sensitive cancer cells by acridine orange staining and confocal microspectrofluorometry. J Histochem Cytochem 45:1255–1264.

Moriyama Y, Manabe T, Yoshimori T, Tashiro Y, M Futai. 1994. ATP-dependent uptake of anti-neoplastic agents by acidic organelles. J Biochem 115:213–218.

Ohkuma S, Poole B. 1978. Fluorescence probe measurement of the intralysosomal pH in living cells and the perturbation of pH by various agents. Proc Natl Acad Sci USA 75:3327–3331.

Presley JF, Mayor S, Dunn KW, Johnson LS, McGraw TE, Maxfield FR. 1993. The End2 mutation in CHO cells slows the exit of transferrin receptors from the recycling compartment but bulk membrane recycling is unaffected. J Cell Biol 122:1231–1241.

Presley JF, Mayor S, McGraw TE, Dunn KW, Maxfield FR. 1997. Bafilomycin A1 treatment retards transferrin receptor recycling more than bulk membrane recycling. J Biol Chem 272:13929–13936.

Roepe PD. 1992. Analysis of the steady-state and initial rate of doxorubicin efflux from a series of multidrug-resistant cells expressing different levels of P-glycoprotein. Biochemistry 31:12555–12564.

Ruetz S, Gros P. 1994. A mechanism for P-glycoprotein action in multidrug resistance: are we there yet? Trends Pharmacol Sci 15: 260–263.

Rutherford AV, Willingham MC. 1993. Ultrastructural localization of daunomycin in multidrug-resistant cultured cells with modulation of the multidrug transporter. J Histochem Cytochem 41:1573–1577.

Scheper RJ, Broxterman HJ, Scheffer GL, Kaaijk P, Dalton WS, van Heijningen TH, van Kalken CK, Slovak ML, de Vries EG, van der Valk P. 1993. Overexpression of a M(r) 110,000 vesicular protein in non-P-glycoprotein-mediated multidrug resistance. Cancer Res 53: 1475–1479.

Schindler M, Grabski S, Hoff E, Simon SM. 1996. Defective pH regulation of acidic compartments in human breast cancer cells (MCF-7) is normalized in adriamycin-resistant cells (MCF-7adr). Biochemistry 35:2811–2817.

Sehested M, Skovsgaard T, van Deurs B, Winther-Nielsen H. 1987a. Increase in nonspecific adsorptive endocytosis in anthracycline- and vinca alkaloid-resistant Ehrlich ascites tumor cell lines. J Natl Cancer Inst 78:171–179.

Sehested M, Skovsgaard T, van Deurs B, Winther-Nielsen H. 1987b. Increased plasma membrane traffic in daunorubicin resistant P388 leukaemic cells. Effect of daunorubicin and verapamil. Br J Cancer 56:747–751.

Seidel A, Hasmann M, Loser R, Bunge A, Schaefer B, Herzig I, Steidtmann K, Dietel M. 1995. Intracellular localization, vesicular accumulation and kinetics of daunorubicin in sensitive and multidrug-resistant gastric carcinoma EPG85–257 cells. Virchows Archiv 426:249–256.

Shapiro AB, Fox K, Lee P, YD Yang, Ling V. 1998. Functional intracellular P-glycoprotein. Int J Cancer 76:857–864.

Simon S, Roy D, Schindler M. 1994. Intracellular pH and the control of multidrug resistance. Proc Natl Acad Sci USA 91:1128–1132.

Simon SM, Schindler M. 1994. Cell biological mechanisms of multidrug resistance in tumors. Proc Natl Acad Sci USA 91:3497–3504.

Sipe DM, Jesurum A, Murphy RF. 1991. Absence of Na+,K(+)-ATPase regulation of endosomal acidification in K562 erythroleukemia cells. Analysis via inhibition of transferrin recycling by low temperatures. J Biol Chem 266:3469–3474.

Sognier MA., Zhang Y, Eberle RL, Belli JA. 1992. Characterization of adriamycin-resistant and radiation-sensitive Chinese hamster cell lines. Biochem Pharmacol 44:1859–1868.

Sognier MA, Zhang Y, Eberle RL, Sweet KM, Altenberg GA, Belli JA. 1994. Sequestration of doxorubicin in vesicles in a multidrug-resistant cell line (LZ-100). Biochem Pharmacol 48:391–401.

Swanson J. 1989. Fluorescent labeling of endocytic compartments. Meth Cell Biol 29:137–151.

Thiebaut F, Currier SJ, Whitaker J, Haugland RP, Gottesman MM, Pastan I, Willingham MC. 1990. Activity of the multidrug transporter results in alkalinization of the cytosol: measurement of cytosolic pH by microinjection of a pH-sensitive dye. J Histochem Cytochem 38:685–690.

Valverde MA., Diaz M, Sepulveda FV, Gill DR, Hyde SC, Higgins CF. 1992. Volume-regulated chloride channels associated with the human multidrug-resistance P-glycoprotein. Nature 355:830–833.

Van Dyke RW. 1986. Anion inhibition of the proton pump in rat liver multivesicular bodies. J Biol Chem 261:15941–15948.

van Weert AW, Dunn KW, Gueze HJ, Maxfield FR, Stoorvogel W. 1995. Transport from late endosomes to lysosomes, but not sorting of integral membrane proteins in endosomes, depends on the vacuolar proton pump. J Cell Biol 130:821–834.

Wadkins RM, Roepe PD. 1997. Biophysical aspects of P-glycoprotein-mediated multidrug resistance. Int Rev Cytol 171:121–165.

Ward DM, Leslie JD, Kaplan J. 1997. Homotypic lysosome fusion in macrophages: analysis using an in vitro assay. J Cell Biol 139:665–673.

Warren L, Jardillier JC, Ordentlich P. 1991. Secretion of lysosomal enzymes by drug-sensitive and multiple drug-resistant cells. Cancer Res 51:1996–2001.

Willingham MC, Cornwell MM, Cardarelli CO, Gottesman MM, Pastan I. 1986. Single cell analysis of daunomycin uptake and efflux in multidrug-resistant and -sensitive KB cells: effects of verapamil and other drugs. Cancer Res 46:5941–5946.

Yamashiro DJ, Tycko B, Fluss SR, Maxfield FR. 1984. Segregation of transferrin to a mildly acidic (pH 6.5) para-Golgi compartment in the recycling pathway. Cell 37:789–800.

Zamora JM, Beck WT. 1986. Chloroquine enhancement of anticancer drug cytotoxicity in multiple drug resistant human leukemic cells. Biochem Pharmacol 35:4303–4310.

Zen K, Biwersi J, Periasamy N, Verkman AS. 1992. Second messengers regulate endosomal acidification in Swiss 3T3 fibroblasts. J Cell Biol 119:99–110.